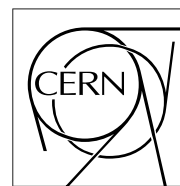


The Compact Muon Solenoid Experiment

CMS Note

Mailing address: CMS CERN, CH-1211 GENEVA 23, Switzerland



20 October 1997

B_s decay vertex resolution

A. Starodumov^{a)}, Z. Xie^{b)}

INFN, Pisa, Italy

Abstract

The resolution of the B_s decay vertex in the channel $B_s^0 \rightarrow D_s^- \pi^+ \rightarrow \phi \pi^- \pi^+ \rightarrow K^+ K^- \pi^- \pi^+$ is evaluated. Full simulation of the decay channel is performed using CMSIM v.112 package. The CMS vertex detector for low luminosity operation with a first pixel layer at $R = 3.8cm$ is assumed. The parameterisation of the secondary vertex resolution is done versus the transverse momentum of B_s .

^{a)} On leave from ITEP, Moscow, Russia

^{b)} also Scuola Normale Superiore, Pisa, Italy

1 Introduction

One of the most promising channel for the $B_s - \bar{B}_s$ oscillation study [1] is the following:

$$B_s^0 \rightarrow D_s^- \pi^+ \rightarrow \phi \pi^- \pi^+ \rightarrow K^+ K^- \pi^- \pi^+ \quad (1)$$

The channel is very challenging since only one charged track (π) comes from the B_s decay vertex. This vertex can be reconstructed only if D_s decay vertex is reconstructed as well. The algorithm used in the study minimises χ^2 of the simultaneous fit of the two vertices. In this Note we study the decay vertex resolution which can be obtained with the CMS tracker.

The note is organised as follows. In Section 2 we describe the event sample used in the study. Results of secondary vertex reconstruction using CMSIM package is shown in Section 3. Parameterisation of the secondary vertex resolution versus transverse momentum of B_s is done in Section 4. In Section 5 we discuss results and make conclusion.

2 Event sample

Proton-proton collisions at centre of mass energy of 14 TeV have been simulated using PYTHIA 5.7 event generator [2]. Both mechanisms of heavy quark production, gluon splitting and fusion, are taken into account. About 10^6 $b\bar{b}$ events have been selected and stored (for the details of the simulation procedure see [3]). Simulation of each event is stopped at the parton level.

Each $b\bar{b}$ event hadronised, fragmented and decayed 5 times to get reasonable statistics of selected B_s mesons. Decay channels of both B mesons have been forced: one B decays into $\mu + X$ (in the study a muon tagging technique is used) and B_s decays according to the equation (1) The collected statistics corresponds to one month of LHC operation assuming integrated luminosity of $L = 10^4 pb^{-1}$ and total $b\bar{b}$ cross-section $\sigma_{b\bar{b}} = 500 \mu b$.

Fig. 1 shows p_t distributions of B_s mesons and final state hadrons after the kinematical selection described in Section 3.2. Because of different initial random number used to hadronise and decay the same event 5 times, no any bias is introduced during this procedure. Fig. 1 illustrates that there is no artificial statistical fluctuations in the transverse momentum spectra.

3 Secondary vertex reconstruction

3.1 How to fit B_s decay vertex

To investigate the B_s oscillation one should measure the proper time of B_s . This is calculated according to the following formula:

$$t = m \times L/p \quad (2)$$

where t is the proper time, m is the mass, p is the momentum and L is the flight path of B_s .

The most important term in this formula is the flight path. The precision of the flight path mainly depends on the precision of the B_s decay vertex reconstruction. In decay (1) only one track (π) comes from the B_s itself, while the other tracks come from the D_s . To reconstruct the B_s decay vertex one needs to reconstruct D_s decay vertex as well. In the study two vertices have been reconstructed in space simultaneously by minimising the following expression:

$$\chi^2 = \sum \frac{d_i^2(X_B, Y_B, Z_B, a)}{\sigma_i^2} \quad (3)$$

Here $i = 1 \div 4$; d_i is a distance from track i to the corresponding decay vertex: for $i = 1$ it is the B_s decay vertex, for $i = 2 \div 4$ it is the D_s decay vertex; σ_i are impact parameter errors, which come from track fitting and are treated separately in the $r - \phi$ and $r - z$ planes, a is the distance between the B_s and D_s decay vertices, which satisfies the following equation:

$$\vec{X}_{D_s} = \vec{X}_{B_s} + a \frac{\vec{P}_{D_s}}{|P_{D_s}|} \quad (4)$$

Here, \vec{P}_{D_s} is the reconstructed momentum of D_s , \vec{X}_{B_s} and \vec{X}_{D_s} three-vectors of B_s and D_s decay vertices respectively.

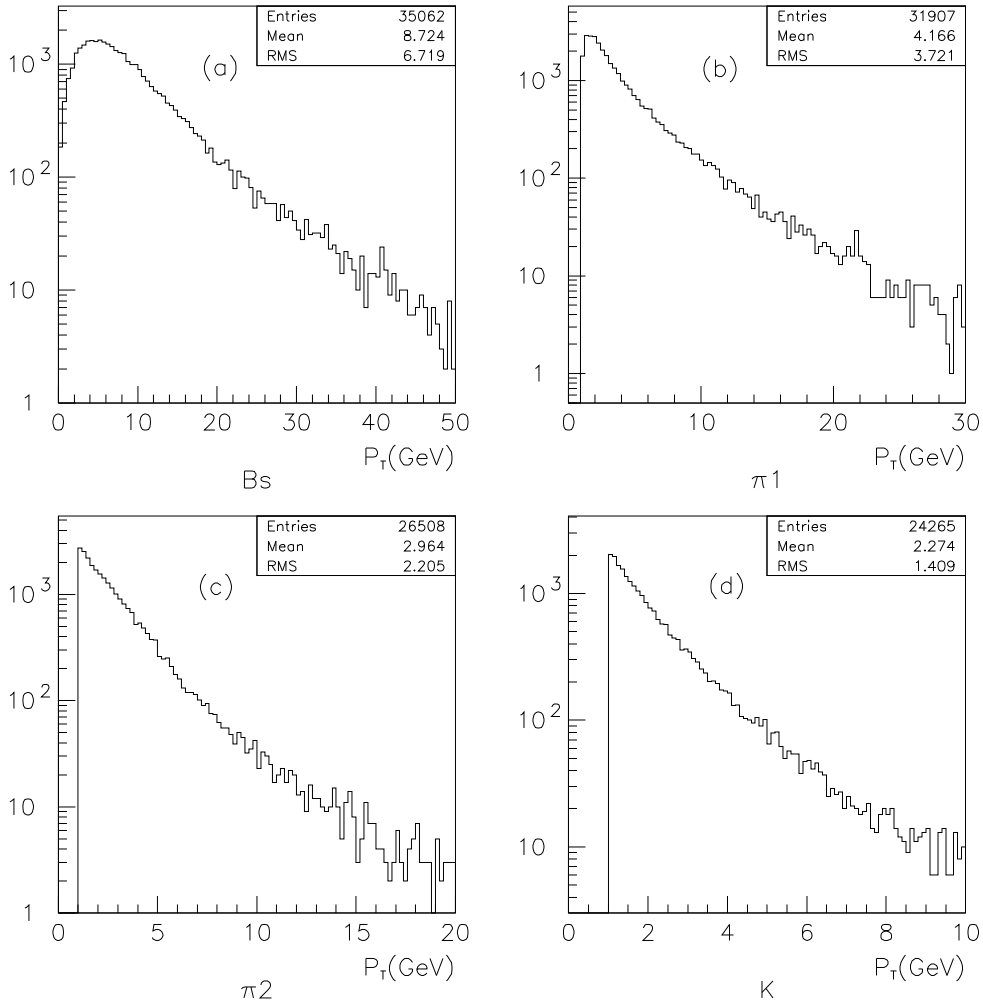


Figure 1: p_t distribution of B_s (a) and final state hadrons: $\pi 1$ (b) is the pion from B_s decay, $\pi 2$ (c) is the pion from D_s decay, K (d) comes from the ϕ decay.

3.2 Selection of events

Track reconstruction and vertex fitting have been done using CMSIM v.112 [4]. CMS tracker Version 3 is used in the study with low luminosity option of pixel detectors (GEOM control card is 'PXLX' 23). For track finding Monte-Carlo method (RECO control card is 'TRAK' 1) is used. MC method means that for the track fitting hits from the real simulated track are used. So, possible pattern recognition problems are ignored in this study. The following kinematical and selection criteria have been applied:

- $|\eta| \leq 2.4$ for all particles;
- $p_t \geq 1\text{GeV}$ for all hadrons (Fig. 1 b ÷ d);
- single muon trigger with the threshold of $p_t \geq 6\text{GeV}$;
- 2 hits in pixel layers for each track (1 hit/layer) \equiv good tracks;
- only events with 4 good tracks from B_s decay are used for vertex fit;
- χ^2 of the vertices fit is less than 20 (Fig. 2 a).

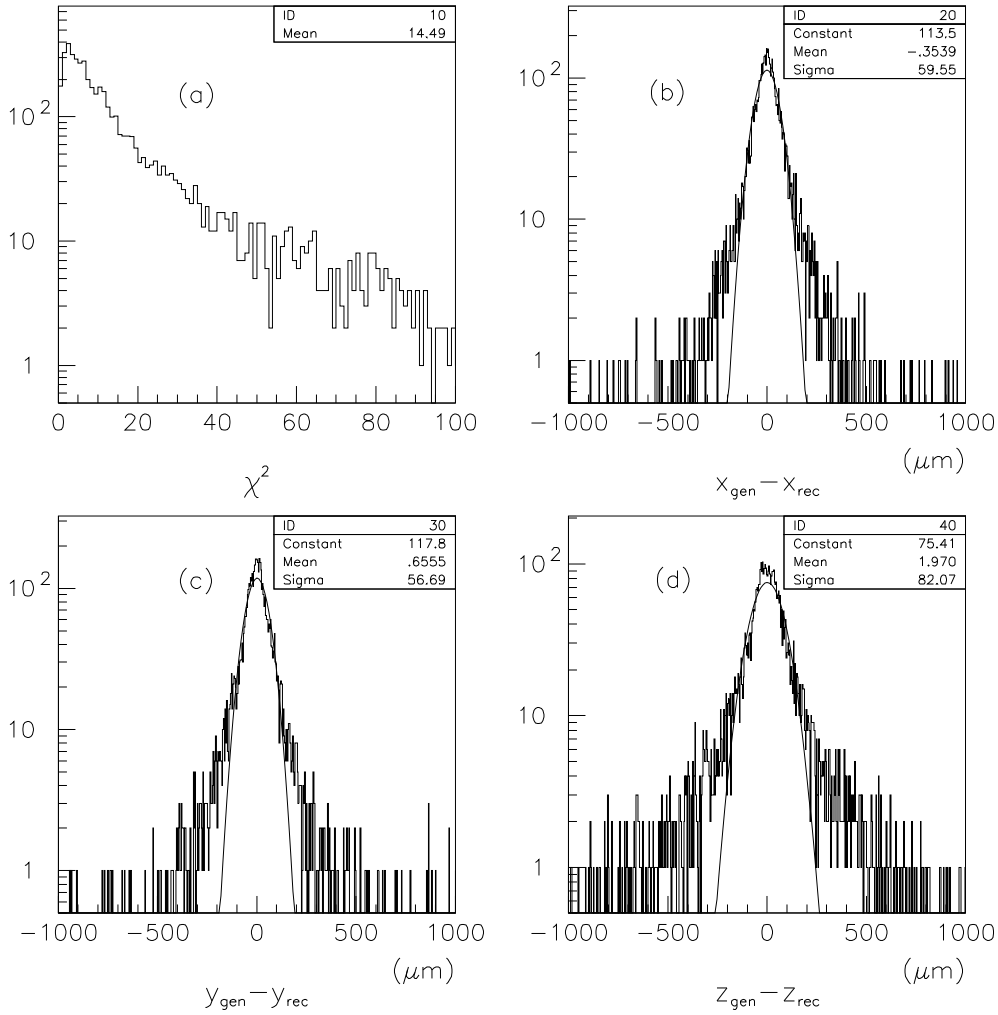


Figure 2: χ^2 of the vertex fit (a) and residuals of the B_s decay vertex in x (b), y (c), z (d) directions

3.3 Result of the B_s decay vertex fit

The fitting procedure returns reconstructed vertices and χ^2 of the fit, but not the errors of the fit. To estimate a secondary vertex resolution one can plot the difference between reconstructed and simulated values. Fig. 2b ÷ d shows residuals of the B_s decay vertex in the x , y and z directions. The Gaussian fit of these distributions provides secondary vertex resolution which is $\sim 60\mu m$ in the x and y directions and $\sim 80\mu m$ in the z direction. To evaluate the error of proper time one has to find a projection of the error on the flight path direction. Fig. 3 illustrates flight path, the errors of the secondary vertex along the flight path (in the $r - \phi$ plane and in space) and in the perpendicular direction. The error along the B_s flight path is about $\sim 77/115\mu m$ in the transverse plane and in space respectively. The error in the direction which is perpendicular to the flight path is quite small $\sim 20/36\mu m$ in the transverse plane and space respectively. In Section 4 secondary vertex resolution along the transverse flight path of B_s will be parametrised versus p_t of B_s .

4 Parametrisation of the secondary vertex resolution

The difference between generated and reconstructed decay vertex of B_s divided by flight path (relative error) in the transverse plane can be parametrised with two Gaussian. A narrow Gaussian (G1) reflects the resolution of the tracker system and a wide Gaussian (G2) presents 'non-Gaussian' tails. The parametrisation is done with the

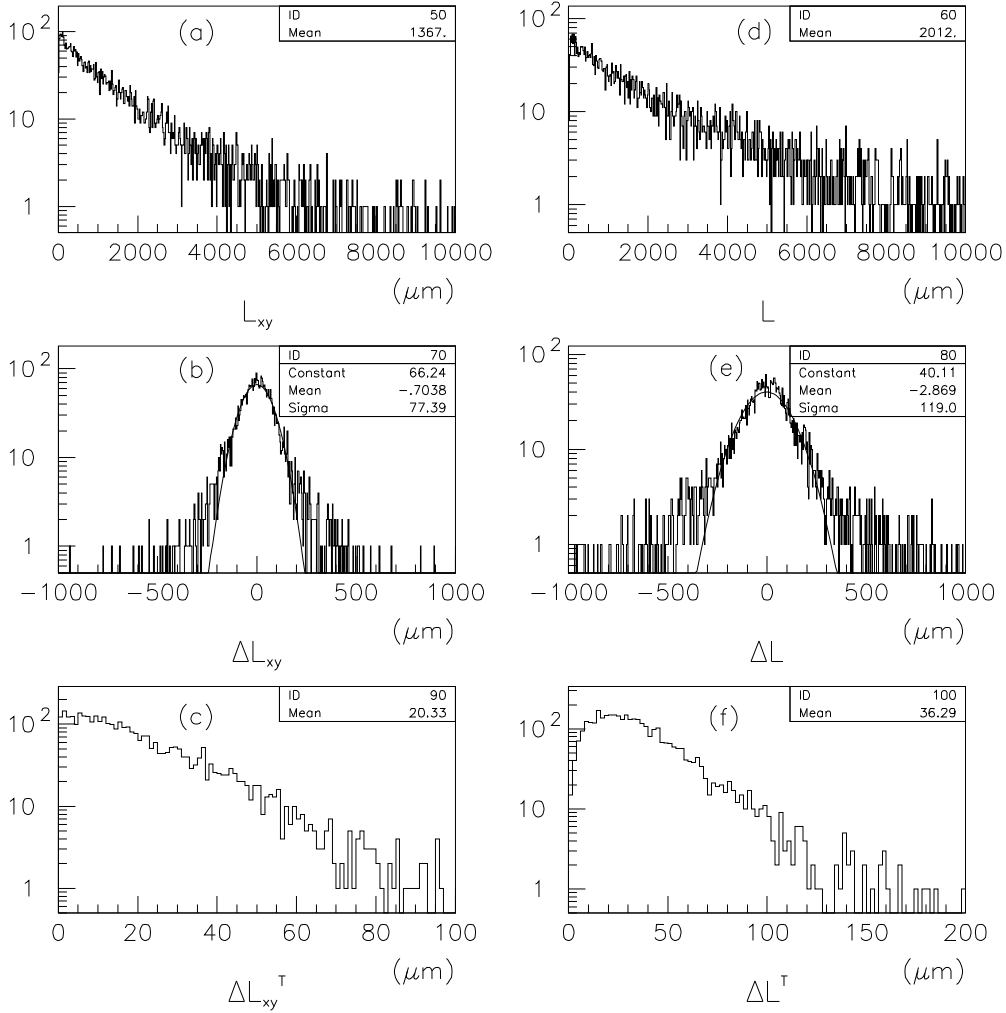


Figure 3: Flight path (L , L_{xy}) and the errors of secondary vertex along (ΔL_{xy} , ΔL) and perpendicular (ΔL_{xy}^T , ΔL^T) to the flight path. On the left ($a \div c$): distributions are in the transverse plane, on the right ($d \div f$): in space.

following functions:

$$P_i = A_i \exp\left(-\frac{(x - \mu_i)^2}{2\sigma_i^2}\right) \quad (5)$$

where $i = 1, 2$ corresponds to narrow and wide Gaussian distributions, respectively.

To parameterise the relative error the full range of the transverse momentum of B_s has been divided in five regions: $\leq 10 GeV$, $10 \div 12 GeV$, $12 \div 16 GeV$, $16 \div 24 GeV$ and $24 \div 40 GeV$. On Fig. 4 one can see the fit of the relative error with a function 'G1+G2' for the full region and the first three regions of transverse momentum of B_s . The regions have been chosen to have approximately the same number of events in each of them. The width of the narrow Gaussian depends on transverse momentum of B_s and varies from 6.5% to 4% while the width of wide Gaussian stays almost constant at the level of 32%-34%. Fig. 5 shows the parametrisation of the narrow Gaussian versus transverse momentum of B_s . The function used for the parametrisation is the following:

$$\frac{\sigma_t}{L_{xy}} = \sqrt{\left(\frac{P_1}{p_t}\right)^2 + P_2^2} \quad (6)$$

Here, σ_t is the error of the flight path in the transverse plane, L_{xy} is the transverse flight path, p_t is the transverse momentum of B_s , P_1 and P_2 are parameters of the fit. Parameter P_2 has the meaning of an asymptotic resolution.

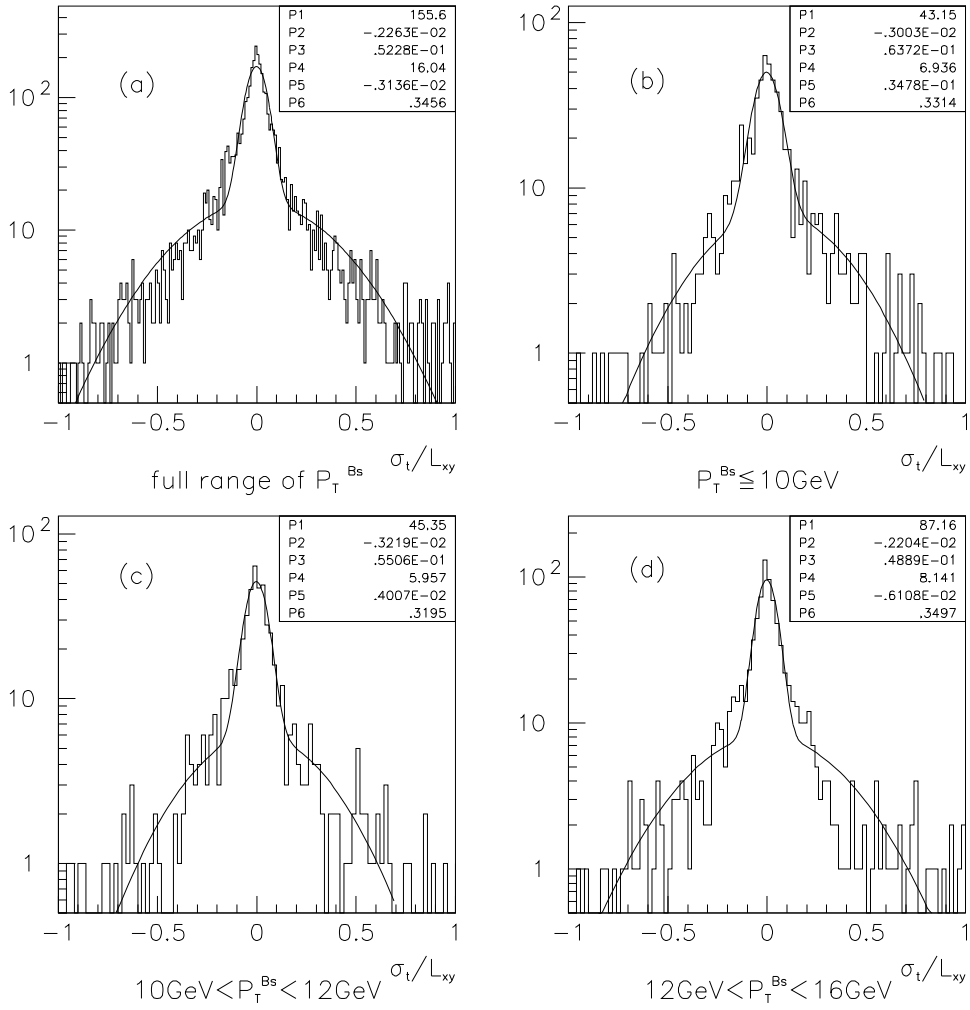


Figure 4: Fitted relative flight path error distributions for full (a) and the first three ranges of P_t of B_s (b ÷ d).

For the CMS tracker in the low luminosity option for the vertex detector (the radius of the first pixel layer in the barrel is 3.8cm) the asymptotic resolution in the transverse plane is about 4%.

To simulate the reconstruction of the B_s decay vertex in the channel (1) one needs to count on the wide Gaussian. The relative fraction of narrow and wide Gaussian can be determined by calculating the ratio of the integrals:

$$I_i = \int P_i dx = \int A_i \exp\left(-\frac{(x - \mu_i)^2}{2\sigma_i^2}\right) dx \quad (7)$$

which is equal to:

$$\frac{I_1}{I_2} = \sqrt{2\pi} \frac{A_1}{A_2} \frac{\sigma_1 \sigma_2}{\sqrt{\sigma_2^2 - \sigma_1^2}} \quad (8)$$

For all considered ranges of the B_s transverse momentum this ratio is almost constant and equal to ~ 1 . The width of the wide Gaussian about 5 times larger than the width of the narrow one.

5 Conclusion

In this Note the parametrisation of the secondary vertex resolution for B_s decay channel (1) is done using the low luminosity option of the CMS vertex detector. Track reconstruction and vertex fitting are performed with CMSIM

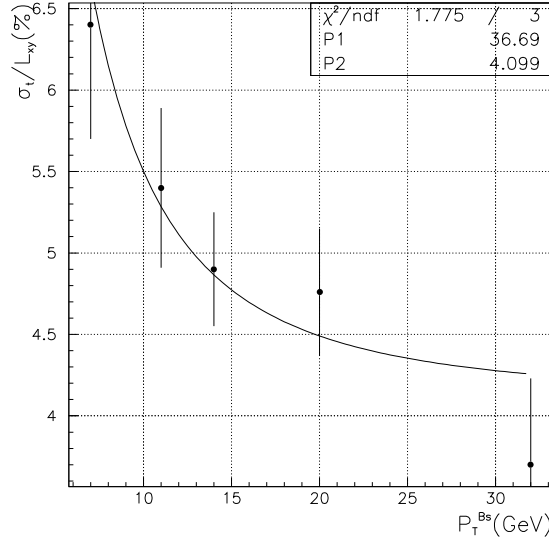


Figure 5: B_s decay vertex resolution versus p_t of B_s .

v.112 package. Secondary vertex resolution can be parametrised as the sum of two Gaussian distributions with the relative fraction of 1:1. The width of the narrow Gaussian can be parametrised with the function (6), where $P1= 37\%$ and $P2= 4\%$. The width of the wide Gaussian is about 5 times bigger than the width of the narrow one.

The asymptotic secondary vertex resolution of 4% is comparable with the resolutions estimated by LHC-B ($\sim 3\%$ [5]) and ATLAS ($\sim 4.5\%$ [6]) Collaborations.

Such a good performance the CMS vertex detector and the whole tracker provides a possibility to measure x_s value up to upper limit (about 30) predicted by the Standard Model [7] in the decay channel (1).

6 Acknowledgement

We would like to thank G.Tonelli for many useful advises and remarks made during the preparation of this Note. We also want to acknowledge R.Castaldi for his attention to this work.

References

- [1] **Proceedings of the XI Symposium of Hadron Collider Physics, World Scientific, 1997**, A.Starodumov, " B_s oscillations and CP-violation at LHC".
- [2] **Computer Physics Commun. 82 (1994) 74**, T.Sjostrand, "PYTHIA 5.7 and JETSET 7.4".
- [3] **Users Manual**, M.Konecki and A.Starodumov, " $b\bar{b}$ Events Simulation Package".
- [4] **Users Guide and Reference Manual**, CMS detector simulation software group, "*CMS Simulation Package*".
- [5] **CERN/LHCC 95-5**, LHC-B, "*Letter of Intent*".
- [6] **ATLAS Internal Note, Physics note no. 095; hep-ex/96110001**, S.Gadomski, P.Eerola and A.V.Bannikov, "*ATLAS sensitivity range for the x_s measurement*".
- [7] **Nuclear Physics B (Proc. Suppl.) 54A (1997) 297**, A.Ali and D.London, "*CP Violation and Flavour Mixing in the Standard Model - 1996 Update*"